

# New Atmospheric O<sub>2</sub>/N<sub>2</sub> Ratio Measurements over the Western North Pacific Using a Cargo Aircraft C-130H

Shigeyuki Ishidoya<sup>1</sup>, Kazuhiro Tsuboi<sup>2</sup>, Hidekazu Matsueda<sup>2</sup>, Shohei Murayama<sup>1</sup>, Shoichi Taguchi<sup>1</sup>, Yousuke Sawa<sup>2</sup>, Yosuke Niwa<sup>2</sup>, Kazuyuki Saito<sup>3</sup>, Kentaro Tsuji<sup>3</sup>, Hidehiro Nishi<sup>3</sup>, Yusuke Baba<sup>3</sup>, Shinya Takatsuji<sup>3</sup>, Koshiro Dehara<sup>3</sup>, and Hiroaki Fujiwara<sup>3</sup>

<sup>1</sup>National Institute of Advanced Industrial Science and Technology (AIST), Tsukuba, Japan

<sup>2</sup>Meteorological Research Institute, Tsukuba, Japan

<sup>3</sup>Japan Meteorological Agency, Tokyo, Japan

## Abstract

Air samples collected over the western North Pacific using a cargo aircraft C-130H have been analyzed for O<sub>2</sub>/N<sub>2</sub> ratio ( $\delta(\text{O}_2/\text{N}_2)$ ), Ar/N<sub>2</sub> ratio ( $\delta(\text{Ar}/\text{N}_2)$ ),  $\delta^{15}\text{N}$  of N<sub>2</sub>,  $\delta^{18}\text{O}$  of O<sub>2</sub> and  $\delta^{40}\text{Ar}$  since May 2012. The relationships of  $\delta(\text{Ar}/\text{N}_2)$ ,  $\delta^{18}\text{O}$  and  $\delta^{40}\text{Ar}$  with  $\delta^{15}\text{N}$  indicate a significant artificial fractionation due to thermal diffusion during the air sample collection. The observed  $\delta(\text{O}_2/\text{N}_2)$  and the atmospheric potential oxygen (APO = O<sub>2</sub> + 1.1 × CO<sub>2</sub>), corrected for the artificial fractionation, show clear seasonal cycles at all altitudes over Minamitorishima, with amplitudes decreasing with height. Both the seasonal amplitude of the mid-tropospheric APO and its ratio to the surface value are found to decrease significantly from the mid-latitude to the subtropical region. The amplitude of the mid-tropospheric CO<sub>2</sub> seasonal cycle does not change significantly meridionally in a latitude band.

(Citation: Ishidoya, S., K. Tsuboi, H. Matsueda, S. Murayama, S. Taguchi, Y. Sawa, Y. Niwa, K. Saito, K. Tsuji, H. Nishi, Y. Baba, S. Takatsuji, K. Dehara, and H. Fujiwara, 2014: New atmospheric O<sub>2</sub>/N<sub>2</sub> ratio measurements over the western North Pacific using a cargo aircraft C-130H. *SOLA*, **10**, 23–28, doi:10.2151/sola.2014-006).

## 1. Introduction

The atmospheric O<sub>2</sub>/N<sub>2</sub> ratio has been observed since the early 1990s to estimate terrestrial biospheric and oceanic CO<sub>2</sub> uptake (Keeling and Shertz 1992). Many observations of the O<sub>2</sub>/N<sub>2</sub> ratio have been carried out at various surface stations throughout the world and on some commercial cargo ships (e.g., Bender et al. 2005; Manning and Keeling 2006; Ishidoya et al. 2012a; Tohjima et al. 2012). However, aircraft observations of the O<sub>2</sub>/N<sub>2</sub> ratio in the free troposphere, as well as its vertical profile measurements, are very limited (Langenfelds et al. 1999; Sturm et al., 2005; Stephens et al. 2009; Ishidoya et al. 2012b). The aircraft observation of the O<sub>2</sub>/N<sub>2</sub> ratio is considered to be useful not only to obtain a greater insight into various carbon exchange processes over a wider geographical area, but also to evaluate three-dimensional transport processes of the air-sea O<sub>2</sub> flux.

For a precise observation of the O<sub>2</sub>/N<sub>2</sub> ratio using aircraft, a quantitative evaluation of various artificial fractionations is needed. Keeling et al. (1998) reported that gradients of pressure, temperature and water vapor in an air sampling system would cause a fractionation of air molecules as a function of their molecular masses. A branching of air at a tee junction in a sample-air flow path could also cause fractionation (e.g. Stephens et al. 2003, 2007). In past studies, the Ar/N<sub>2</sub> ratio, as well as its relationship with the stable isotopic ratios of N<sub>2</sub>, O<sub>2</sub> and Ar, was used to eval-

uate the thermally-diffusive fractionation effect due to radiative heating/cooling at the air intake (Blaine et al. 2006; Sturm et al. 2006; Ishidoya et al. 2013).

Taking these considerations into account, we have conducted a systematic observation of the O<sub>2</sub>/N<sub>2</sub> ratio in the free troposphere over the western North Pacific by using a cargo aircraft C-130H. To evaluate the possible effects of the artificial O<sub>2</sub> and N<sub>2</sub> fractionations on the O<sub>2</sub>/N<sub>2</sub> ratio, we have also made precise measurements of the Ar/N<sub>2</sub> ratio, along with the stable isotopic ratios of N<sub>2</sub>, O<sub>2</sub> and Ar. In this paper, we present a correction method of the artificial fractionation, and then discuss time and space variations of the corrected O<sub>2</sub>/N<sub>2</sub> ratio.

## 2. Method

The cargo aircraft C-130H flies once per month from Atsugi Base (35.45°N, 139.45°E), Kanagawa, Japan, to Minamitorishima (MNM; 24.28°N, 153.98°E), a small and isolated coral island located 1,850 km southeast of Tokyo, Japan. The flight route of the C-130H aircraft is shown in Fig. 1. The flight altitude is about 6 km and the flight time is about 4 hours. During the flight, 24 air samples are pressurized into 1.7 L titanium flasks whose inner walls are silica-coated to an absolute pressure of 0.4 MPa. A set of 17–20 samples are collected during the level flight and others are obtained during the descent portion at MNM. Details of the air sampling protocol using the C-130H has been described elsewhere (Tsuboi et al. 2013; Niwa et al. 2014). Additional 6 air samples are also collected using the similar flasks at the MNM ground surface during the time period of the C-130H flight. The flask air samples are brought back to the Japan Meteorological Agency (JMA)

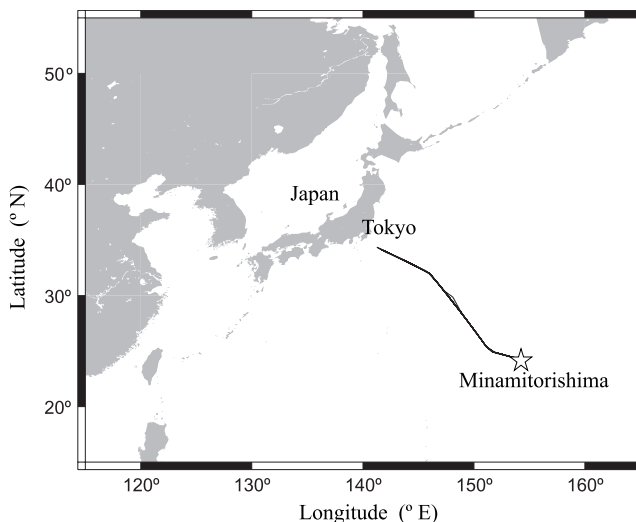


Fig. 1. Flight route of the cargo aircraft C-130H for the period May 2012–April 2013.

Corresponding author: Shigeyuki Ishidoya, Research Institute for Environmental Management Technology, National Institute of Advanced Industrial Science and Technology (AIST), AIST Tsukuba West, 16-1 Onogawa, Tsukuba, Ibaraki 305-8569, Japan. E-mail: s-ishidoya@aist.go.jp. ©2014, the Meteorological Society of Japan.

and analyzed for the CO<sub>2</sub>, CH<sub>4</sub>, CO and N<sub>2</sub>O concentration. The CO<sub>2</sub> concentration reported here has been measured using a non-dispersive infrared analyzer (Licor, LI-7000) with a precision of less than ±0.07 ppm (Tsuboi et al. 2013). The dataset is posted on the WMO's World Data Centre for Greenhouse Gases (WMO/WGCGG, <http://ds.data.jma.go.jp/gmd/wdgg/wdgg.html>).

After the JMA analyses, the flasks are sent to the National Institute of Advanced Industrial Science and Technology (AIST) to measure the O<sub>2</sub>/N<sub>2</sub> and Ar/N<sub>2</sub> ratios, as well as the stable isotopic ratios of N<sub>2</sub>, O<sub>2</sub> and Ar. In this study, we have analyzed the air samples (a total 305 samples) collected over the period May 2012–April 2013. The values of δ(O<sub>2</sub>/N<sub>2</sub>), δ(Ar/N<sub>2</sub>), stable isotopic ratios of N<sub>2</sub>, O<sub>2</sub> and Ar (δ<sup>15</sup>N, δ<sup>18</sup>O and δ<sup>40</sup>Ar) are reported in this study as:

$$\delta(^{16}\text{O}^{16}\text{O}/^{14}\text{N}^{14}\text{N}) = \left[ \frac{(^{16}\text{O}^{16}\text{O}/^{14}\text{N}^{14}\text{N})_{\text{sample}}}{(^{16}\text{O}^{16}\text{O}/^{14}\text{N}^{14}\text{N})_{\text{standard}}} - 1 \right] \times 10^6, \quad (\text{per meg}) \quad (1)$$

$$\delta(^{40}\text{Ar}/^{14}\text{N}^{14}\text{N}) = \left[ \frac{(^{40}\text{Ar}/^{14}\text{N}^{14}\text{N})_{\text{sample}}}{(^{40}\text{Ar}/^{14}\text{N}^{14}\text{N})_{\text{standard}}} - 1 \right] \times 10^6 \quad (\text{per meg}), \quad (2)$$

$$\delta^{15}\text{N} = \left[ \frac{(^{15}\text{N}^{14}\text{N}/^{14}\text{N}^{14}\text{N})_{\text{sample}}}{(^{15}\text{N}^{14}\text{N}/^{14}\text{N}^{14}\text{N})_{\text{standard}}} - 1 \right] \times 10^6 \quad (\text{per meg}), \quad (3)$$

$$\delta^{18}\text{O} = \left[ \frac{(^{18}\text{O}^{16}\text{O}/^{16}\text{O}^{16}\text{O})_{\text{sample}}}{(^{18}\text{O}^{16}\text{O}/^{16}\text{O}^{16}\text{O})_{\text{standard}}} - 1 \right] \times 10^6 \quad (\text{per meg}), \quad (4)$$

$$\delta^{40}\text{Ar} = \left[ \frac{(^{40}\text{Ar}/^{36}\text{Ar})_{\text{sample}}}{(^{40}\text{Ar}/^{36}\text{Ar})_{\text{standard}}} - 1 \right] \times 10^6 \quad (\text{per meg}), \quad (5)$$

where the subscripts ‘sample’ and ‘standard’ indicate the values of the sample air and the standard air, respectively. The values of δ(O<sub>2</sub>/N<sub>2</sub>), δ(Ar/N<sub>2</sub>), δ<sup>15</sup>N, δ<sup>18</sup>O and δ<sup>40</sup>Ar of the air samples are determined against our primary standard gas, prepared by drying natural air and then stored in a 48-L high-pressure cylinder (cylinder No. CRC00045), using a mass spectrometer (Thermo Scientific Delta-V) (Ishidoya and Murayama 2014) with a respective reproducibility of ±3.0, ±7.1, ±1.8, ±4.5 and ±33 per meg (±1σ). It is noted that all the uncertainties shown in this study mean ±1σ.

### 3. Results and discussion

#### 3.1 Effect of artificial fractionations of O<sub>2</sub> and N<sub>2</sub> on the observed δ(O<sub>2</sub>/N<sub>2</sub>)

Figure 2 shows the latitudinal distributions of δ(O<sub>2</sub>/N<sub>2</sub>), δ(Ar/N<sub>2</sub>), δ<sup>15</sup>N of N<sub>2</sub> and δ<sup>18</sup>O of O<sub>2</sub> from the C-130H flight on December 2012. All of the measured values vary noticeably with latitude but their distribution patterns are quite similar with one another. Such large geographical variations have been found in all other flights as well. The measured values of δ<sup>15</sup>N and δ<sup>18</sup>O with their ranges of 60–100 per meg are obviously beyond the range of natural variability, which is expected to be nearly constant in the troposphere since turnover times of atmospheric N<sub>2</sub> and O<sub>2</sub> are on the order of 10<sup>7</sup> and 1200 years, respectively (e.g. Bender et al. 1994). In addition, the measured δ(Ar/N<sub>2</sub>) variability of about 800 per meg is also outside the natural range since its small seasonal cycle at the surface driven by the thermally-driven air-sea Ar and N<sub>2</sub> fluxes has a peak-to-peak amplitude of only 10–35 per meg (Keeling et al. 2004; Cassar et al. 2008; Ishidoya and Murayama 2014). It is suggested therefore, that the significant variations of the measured δ(Ar/N<sub>2</sub>), δ<sup>15</sup>N and δ<sup>18</sup>O values are attributable to some kind of artificial fractionations of O<sub>2</sub> and N<sub>2</sub> caused by the flask air sampling onboard the C-130H aircraft.

To evaluate the effects of the fractionation on the measured δ(O<sub>2</sub>/N<sub>2</sub>), we examine the relationships between the values of δ(Ar/

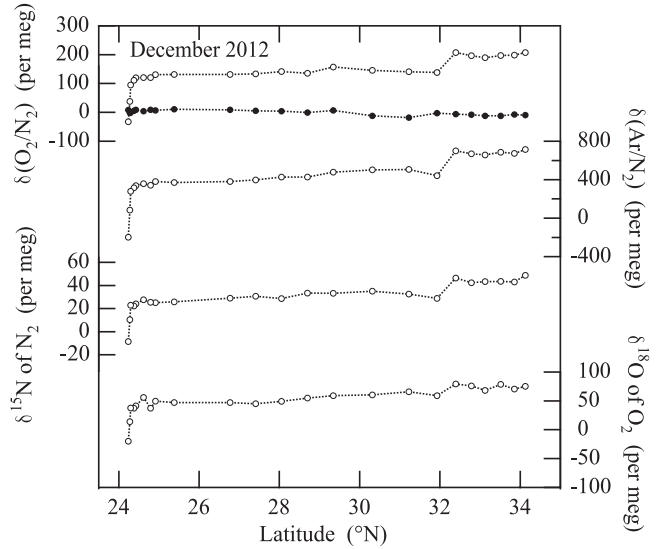


Fig. 2. Typical analytical results of δ(O<sub>2</sub>/N<sub>2</sub>), δ(Ar/N<sub>2</sub>), δ<sup>15</sup>N of N<sub>2</sub> and δ<sup>18</sup>O of O<sub>2</sub> obtained from the air samples collected by the aircraft on December 2012 (open circles). The δ(O<sub>2</sub>/N<sub>2</sub>) values corrected for the thermally-diffusive fractionation of O<sub>2</sub> and N<sub>2</sub> are also shown (filled circles) (see text).

N<sub>2</sub>) and δ<sup>15</sup>N, and δ<sup>18</sup>O and δ<sup>15</sup>N using all the samples collected for this study (Fig. 3). It is found that both δ(Ar/N<sub>2</sub>) and δ<sup>18</sup>O change linearly in proportion to δ<sup>15</sup>N. Their linear regression analyses give slopes of 16.0 ± 0.2 per meg per meg<sup>-1</sup> for the δ(Ar/N<sub>2</sub>)/δ<sup>15</sup>N ratio and 1.49 ± 0.03 per meg per meg<sup>-1</sup> for the δ<sup>18</sup>O/δ<sup>15</sup>N ratio. These ratios are very close to those values (16.2 ± 0.1 for δ(Ar/N<sub>2</sub>)/δ<sup>15</sup>N and 1.55 ± 0.02 for δ<sup>18</sup>O/δ<sup>15</sup>N) determined from the laboratory experiments for the effect of thermal diffusion fractionations on δ(Ar/N<sub>2</sub>), δ<sup>15</sup>N and δ<sup>18</sup>O (Ishidoya et al. 2013). They are clearly different from those expected from the theoretical mass-dependent fractionation due to a gradient of pressure (Keeling et al. 1998) (12 for δ(Ar/N<sub>2</sub>)/δ<sup>15</sup>N and 2 for δ<sup>18</sup>O/δ<sup>15</sup>N). We have also confirmed that the simultaneously-measured δ<sup>40</sup>Ar/δ<sup>15</sup>N ratio (2.51 ± 0.1 per meg per meg<sup>-1</sup>) is also close to that expected from the thermal diffusion experiments (2.75 ± 0.05 per meg per meg<sup>-1</sup>), although the measurement precision of δ<sup>40</sup>Ar is relatively low. Therefore, it is concluded that a fractionation of air molecules occurs in the air sampling onboard the C-130H aircraft due to the thermal diffusion and that its effect could be quantitatively estimated using the results of the above-mentioned laboratory experiments. Although the mechanism how the thermal diffusion fractionation occurs during the air sampling is not clear, it may be related to the fact that the ambient air, supplied from the jet engine of the C-130H to pressurize the cabin, is split into several branches. Since the air samples are collected through one of the branches, the fractionation of air molecules could be attributed to a temperature gradient at the branches (e.g., Stephens et al. 2003, 2007). It is also noted that a weakening of the thermal diffusion fractionation during the descent to MNM is seen from Fig. 2. Therefore, the cause of the thermal diffusion fractionation may also be related to the flight parameters such as ambient pressure and temperature.

Taking these facts into consideration, we have corrected the thermally-diffusive fractionation of O<sub>2</sub> and N<sub>2</sub> superimposed on the observed δ(O<sub>2</sub>/N<sub>2</sub>) using the following equation;

$$\delta(\text{O}_2/\text{N}_2)_{\text{cor.}} = \delta(\text{O}_2/\text{N}_2)_{\text{meas.}} - \alpha_{\text{O}_2} \cdot \alpha_{\text{Ar}}^{-1} \cdot \Delta\delta(\text{Ar}/\text{N}_2)_{\text{meas.}} \quad (\text{per meg}). \quad (6)$$

Here, δ(O<sub>2</sub>/N<sub>2</sub>)<sub>cor.</sub> and δ(O<sub>2</sub>/N<sub>2</sub>)<sub>meas.</sub> denote the corrected and measured δ(O<sub>2</sub>/N<sub>2</sub>), respectively. The coefficients α<sub>O<sub>2</sub></sub> = 4.57 ± 0.02 and α<sub>Ar</sub> = 16.2 ± 0.1 are the δ(O<sub>2</sub>/N<sub>2</sub>)/δ<sup>15</sup>N and δ(Ar/N<sub>2</sub>)/δ<sup>15</sup>N ratios respectively, determined from the experiments on the thermal diffusion fractionation (Ishidoya et al. 2013). Δδ(Ar/N<sub>2</sub>)<sub>meas.</sub> is the deviation of the measured δ(Ar/N<sub>2</sub>) from its reference point. Our choice of the reference point is based on the following argument.

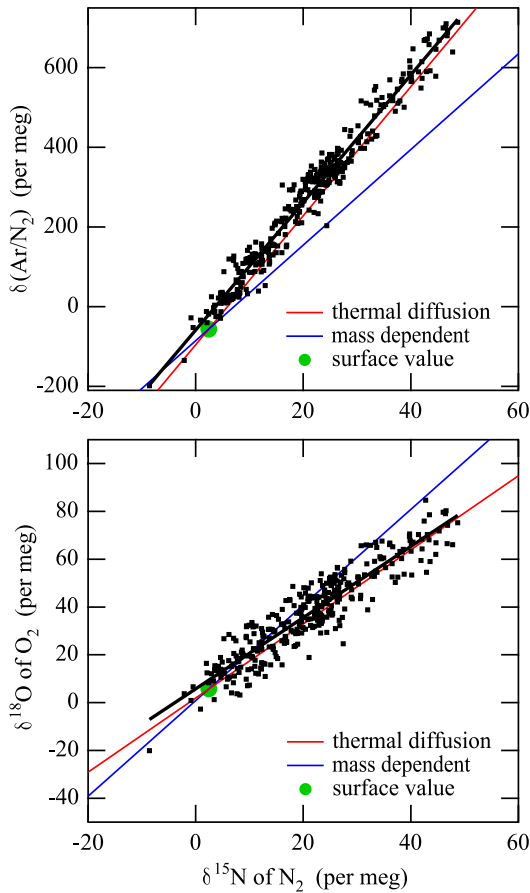


Fig. 3. Relationships of the measured  $\delta(\text{Ar}/\text{N}_2)$  and  $\delta^{18}\text{O}$  of  $\text{O}_2$  with  $\delta^{15}\text{N}$  of  $\text{N}_2$  obtained from the air samples collected on the aircraft and at the surface on Minamitorishima (black dots). Least-square regression lines fitted to the data are also shown (black lines). The relationships expected from the thermally-diffusive and mass-dependent fractionation of air molecules are also shown by red and blue lines, respectively. Green circles denote the annual average surface values of  $\delta^{15}\text{N}$ ,  $\delta(\text{Ar}/\text{N}_2)$  and  $\delta^{18}\text{O}$  observed at Tsukuba ( $36^\circ\text{N}$ ,  $140^\circ\text{E}$ ), Japan.

Both the seasonal and latitudinal variations of the atmospheric  $\delta(\text{Ar}/\text{N}_2)$  are smaller than those of  $\delta(\text{O}_2/\text{N}_2)$ ; the latitudinal difference in the annual mean  $\delta(\text{Ar}/\text{N}_2)$  at the surface stations located in the  $82^\circ\text{N}$ – $90^\circ\text{S}$  latitude zones was observed to be less than  $\pm 5$  per meg (Keeling et al. 2004). Therefore, we use the annual average value of  $\delta(\text{Ar}/\text{N}_2)$  observed at the surface in Tsukuba ( $36^\circ\text{N}$ ,  $140^\circ\text{E}$ ), Japan (Ishidoya and Murayama 2014) as the reference point in calculating  $\Delta\delta(\text{Ar}/\text{N}_2)_{\text{meas}}$ . The uncertainties in the  $\alpha_{\text{O}_2}$  and  $\alpha_{\text{Ar}}$  ( $\pm 0.02$  and  $\pm 0.1$ ) yield uncertainties of less than  $\pm 2.4$  per meg for  $\delta(\text{O}_2/\text{N}_2)_{\text{cor}}$  under the condition that  $\Delta\delta(\text{Ar}/\text{N}_2)_{\text{meas}}$  lies 0–800 per meg. The  $\pm 7.1$  per meg value of the measurement precision of  $\delta(\text{Ar}/\text{N}_2)$  also yields uncertainties of  $\pm 2$  per meg for  $\delta(\text{O}_2/\text{N}_2)_{\text{cor}}$ . Therefore, an overall uncertainty of  $\delta(\text{O}_2/\text{N}_2)_{\text{cor}}$  is estimated to be less than  $\pm 4.3$  per meg, which is small enough to detect variations of interest in atmospheric  $\delta(\text{O}_2/\text{N}_2)$ .

The  $\delta(\text{O}_2/\text{N}_2)_{\text{cor}}$  values obtained in December 2012 are also plotted in Fig. 2, for a comparison with  $\delta(\text{O}_2/\text{N}_2)_{\text{meas}}$ . The maximum correction is found to be about 200 per meg. It should also be noted that  $\delta(\text{Ar}/\text{N}_2)$  shows a small seasonal cycle at the surface around Japan, with a peak-to-peak amplitude of about 16 per meg at Tsukuba (Ishidoya and Murayama 2014). The effect of the seasonal  $\delta(\text{Ar}/\text{N}_2)$  cycle on the  $\delta(\text{O}_2/\text{N}_2)_{\text{cor}}$  is not excluded in this study, although it would lead to an over (under)-correction of the surface  $\delta(\text{O}_2/\text{N}_2)_{\text{cor}}$  by about 2 per meg in the summertime (wintertime).

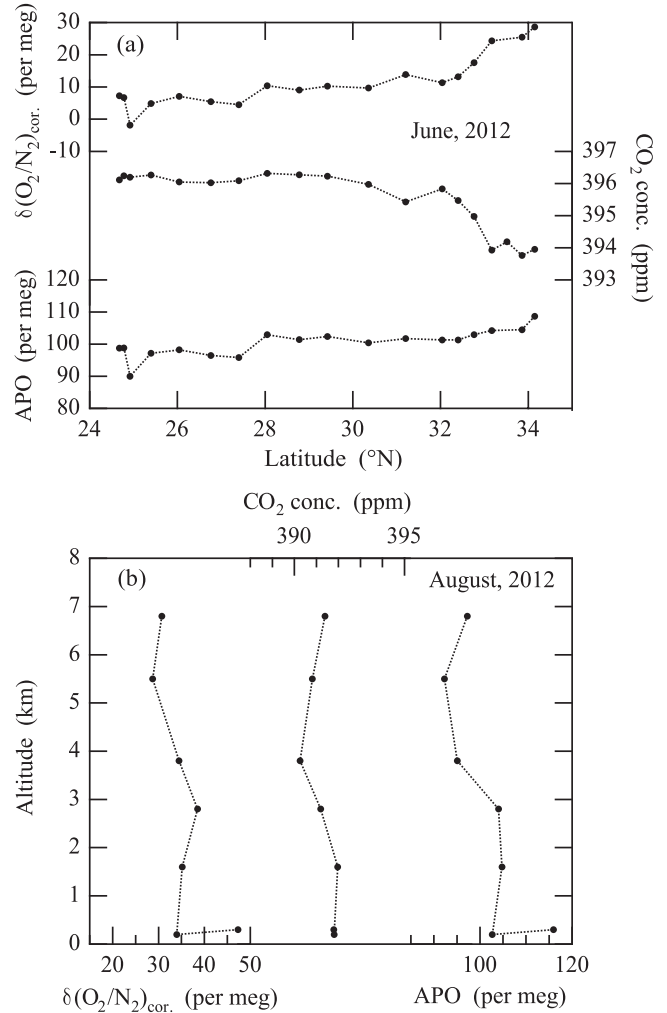


Fig. 4. (a) Latitudinal distribution of  $\delta(\text{O}_2/\text{N}_2)_{\text{cor}}$ ,  $\text{CO}_2$  concentration and APO at height interval between 5.6–6.2 km on June 19, 2012. (b) Vertical profiles of  $\delta(\text{O}_2/\text{N}_2)_{\text{cor}}$ ,  $\text{CO}_2$  concentration and APO on August 20, 2012.

### 3.2 Spatial variation of the $\delta(\text{O}_2/\text{N}_2)$

Figures 4a, b show examples of the latitudinal distributions and the vertical profiles of  $\delta(\text{O}_2/\text{N}_2)_{\text{cor}}$ ,  $\text{CO}_2$  concentration and atmospheric potential oxygen (APO), observed on 19 June and 20 August, 2012, respectively. The parameter APO is a conservative quantity for terrestrial biospheric activities (Stephens et al. 1998) and an indicator of air-sea  $\text{O}_2$  fluxes; it is calculated using the following equation;

$$\text{APO} = \delta(\text{O}_2/\text{N}_2)_{\text{cor}} - 1.1 \times (1/0.20946) \times \text{CO}_2 - 2000 \quad (\text{per meg}). \quad (7)$$

Here, the value 1.1 is the  $-\text{O}_2:\text{CO}_2$  exchange ratio for the terrestrial biospheric activities (Severinghaus 1995), 0.20946 is the mole fraction of  $\text{O}_2$  in the atmosphere (Machta and Hughes 1970) and 2000 is an arbitrary APO reference point. As seen in Fig. 4a, the increasing  $\delta(\text{O}_2/\text{N}_2)_{\text{cor}}$  with decreasing  $\text{CO}_2$  concentration is observed at higher latitudes north of  $33^\circ\text{N}$ . In this region, APO shows no significant changes, suggesting an intrusion of continental air masses influenced by the terrestrial biospheric activities and/or fossil fuel combustions. This conjecture is based on the backward trajectory analysis using the HYSPLIT model (Draxler and Rolph 2003; Rolph 2003; available from NOAA Air Resources Laboratory at [http://ready.arl.noaa.gov/HYSPLIT\\_traj.php](http://ready.arl.noaa.gov/HYSPLIT_traj.php)) showing air parcels rising from the equatorial surface region into the middle troposphere north of  $33^\circ\text{N}$ . These results indicate that the  $\delta(\text{O}_2/\text{N}_2)_{\text{cor}}$  data are able to capture synoptic-scale variations.

Figure 4b shows the vertical profiles of  $\delta(\text{O}_2/\text{N}_2)_{\text{cor.}}$ , CO<sub>2</sub> concentration and APO observed over MNM. The vertical  $\delta(\text{O}_2/\text{N}_2)_{\text{cor.}}$  profile does not anti-correlate with the CO<sub>2</sub> concentration, suggesting weak contributions of the terrestrial biospheric activities and/or fossil fuel combustions. APO below 2.8 km is clearly higher than that above 3.8 km. This difference is associated with a change in the air mass origin, as estimated by the 5-days backward trajectories; air parcels below 2.8 km and above 3.8 km are respectively transported from layers near the surface over the Pacific and upper or middle troposphere. These results suggest significant effects of the summertime sea-to-air O<sub>2</sub> fluxes (Garcia and Keeling 2001) on APO below 2.8 km.

### 3.3 Seasonal variation of the $\delta(\text{O}_2/\text{N}_2)$

Figure 5 shows the time variations of  $\delta(\text{O}_2/\text{N}_2)_{\text{cor.}}$ , CO<sub>2</sub> concentration and APO observed at four vertical layers from the surface to 6.8 km over MNM. Best-fitted curves to the data, consisting of the fundamental and its first harmonics (periods of 12 and 6 months) and a linear trend, are also shown. Since the observation period is too short to derive a reliable secular trend by the curve-fitting, we assume the averaged secular trend values of  $-22.0$  per meg yr<sup>-1</sup>,  $2.09$  ppm yr<sup>-1</sup> and  $-10.9$  per meg yr<sup>-1</sup> over Japan during 2000–2010 (Ishidoya et al. 2012b) for the linear trends of  $\delta(\text{O}_2/\text{N}_2)_{\text{cor.}}$ , CO<sub>2</sub> concentration and APO, respectively.

The seasonal cycles of  $\delta(\text{O}_2/\text{N}_2)_{\text{cor.}}$  and CO<sub>2</sub> concentration vary almost in opposite phase at all altitudes, with their amplitudes reduced and phases delayed with increasing altitude. The seasonal maximum and minimum of  $\delta(\text{O}_2/\text{N}_2)_{\text{cor.}}$  (CO<sub>2</sub> concentration) appear in early to late September and mid-March to mid-April (mid to late September and mid-April), respectively. The peak-to-peak seasonal amplitudes of  $\delta(\text{O}_2/\text{N}_2)_{\text{cor.}}$  (CO<sub>2</sub> concentration) at 0.0–1.7, 1.7–3.4, 3.4–5.1 and 5.1–6.8 km calculated from the fitted curves are 70, 53, 50 and 45 per meg (8.9, 7.7, 7.5 and 7.0 ppm), respectively. The seasonal phase and amplitude of the  $\delta(\text{O}_2/\text{N}_2)_{\text{cor.}}$  cycle in the layer 0.0–1.7 km also agree with the seasonal  $\delta(\text{O}_2/\text{N}_2)_{\text{cor.}}$

cycle observed at the surface MNM (Tohjima, Y., personal communications). On the other hand, the APO seasonal maximum and minimum in the 0.0–1.7 km layer appear nearly 2 months earlier than the CO<sub>2</sub> seasonal minimum and maximum, respectively, while such phase lag is not observed at 5.1–6.8 km. The respective peak-to-peak amplitudes of APO at 0.0–1.7, 1.7–3.4, 3.4–5.1 and 5.1–6.8 km are 37, 20, 15 and 9 per meg, so that the ratios of the seasonal APO amplitude at 1.7–3.4, 3.4–5.1 and 5.1–6.8 km to 0.0–1.7 km are 52, 39 and 24%. These ratios are significantly smaller than those of CO<sub>2</sub> concentration, which are 86, 83 and 78% at 1.7–3.4, 3.4–5.1 and 5.1–6.8 km, respectively. These facts suggest that the seasonal APO cycle near the surface at MNM is strongly affected by the local seasonal air-sea O<sub>2</sub> flux. The observed increase in APO in the early spring also precedes the decrease of CO<sub>2</sub> concentration by about 2 months at Hateruma (24°N, 124°E) located in the same western North Pacific region (Tohjima et al. 2003). Therefore, our observation appears to be typical in the northern subtropical region, reflecting the seasonality of the air-sea O<sub>2</sub> flux in the region.

Figure 5 also shows the annual average values of  $\delta(\text{O}_2/\text{N}_2)_{\text{cor.}}$ , CO<sub>2</sub> concentration and APO at four vertical layers over MNM. The annual  $\delta(\text{O}_2/\text{N}_2)_{\text{cor.}}$  averages increase with increasing altitude, while the CO<sub>2</sub> concentration decreases. This observation suggests that the lower troposphere over MNM is likely affected by a long-range transport of air masses with depleted O<sub>2</sub> and enhanced CO<sub>2</sub> produced by fuel combustions in the East Asia continent. In fact, polluted air masses from the combustion sources over the Asian continent are often observed at MNM (Wada et al. 2011, 2013). The vertical gradients of the annual average values of  $\delta(\text{O}_2/\text{N}_2)_{\text{cor.}}$  and CO<sub>2</sub> concentration could also be attributable to the annual net ocean O<sub>2</sub> sink and CO<sub>2</sub> source around MNM. In this connection, Tohjima et al. (2012) reported the APO trough in the northern mid-latitude near the surface over the western Pacific, and suggested the significant annual net ocean O<sub>2</sub> sink at the region. Therefore, a simulation using an atmospheric transport model, considering both the fossil fuel and the oceanic O<sub>2</sub> and CO<sub>2</sub> fluxes, will be a future task to interpret the vertical profile of the annual average APO over MNM.

Figure 6a shows the time variations of  $\delta(\text{O}_2/\text{N}_2)_{\text{cor.}}$ , CO<sub>2</sub> concentration and APO observed in the 5.1–6.9 km layer at four latitudes between 25.5°N and 33.5°N. Best-fitted curves to the data, consisting of two-harmonics and the similar linear trends to Fig. 5, are also shown. In the following discussion, we focus mainly on the latitudinal differences in the seasonal cycles rather than the annual averages of the observed values since the latitudinal differences in the annual average  $\delta(\text{O}_2/\text{N}_2)_{\text{cor.}}$ , CO<sub>2</sub> concentration and APO are found to be only  $\pm 1.9$  per meg,  $\pm 0.19$  ppm and  $\pm 1.3$  per meg, respectively, and our observation period is only 1 year. Therefore, longer term observations are needed to discuss the latitudinal difference in the annual average middle tropospheric APO climatologically, which would be useful to evaluate the atmospheric transport processes of the air-sea O<sub>2</sub> flux related to the equatorial bulge of the APO (Tohjima et al. 2005, 2012).

The values of  $\delta(\text{O}_2/\text{N}_2)_{\text{cor.}}$  and CO<sub>2</sub> concentration show clear seasonal cycles at all latitudes with summertime maxima and minima, respectively. APO also shows clear seasonal cycles, however, its seasonal amplitude decreases significantly toward the lower latitudes. As seen in Fig. 6b, the seasonal amplitude of the mid-tropospheric APO at 33.5°N is about 3.5 times larger than that observed at 25.5°N. On the other hand, the seasonal CO<sub>2</sub> amplitude does not change significantly from 33.5°N to 25.5°N, consistent with the results reported by Matsueda et al. (2002). The peak-to-peak amplitudes of the seasonal APO cycles near the surface over the western Pacific (Fig. 9 in Tohjima et al. 2012) are about 35, 45 and 55 per meg at 25, 30 and 35°N, respectively, so that the ratios of the seasonal APO amplitude in the middle troposphere to the surface at 25.5, 29.5 and 33.5°N are about 24, 53 and 55%. Ishidoya et al. (2012b) also reported the ratios of the seasonal APO amplitude at 4 km to the surface to be 67% over Sendai (38°N, 140°E), Japan. Therefore, the middle troposphere to the surface ratios of the seasonal APO amplitude are found to decrease significantly with decreasing latitude (Fig. 6b). Such lat-

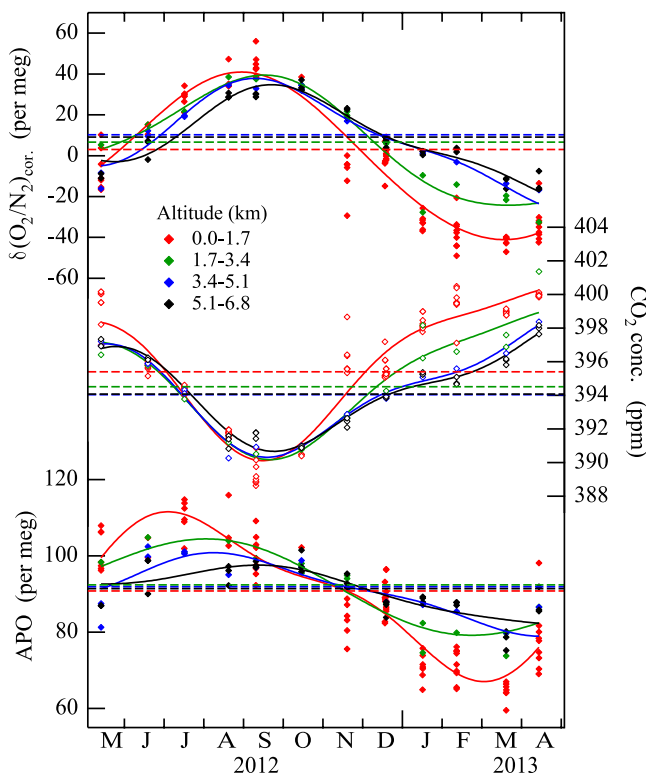


Fig. 5.  $\delta(\text{O}_2/\text{N}_2)_{\text{cor.}}$ , CO<sub>2</sub> concentration and APO observed in the troposphere over Minamitorishima, Japan. Best-fitted curves to the data consist of two-harmonics and specified linear trends are also shown (solid lines, see text). Dashed lines denote the average values of the fitted curves.

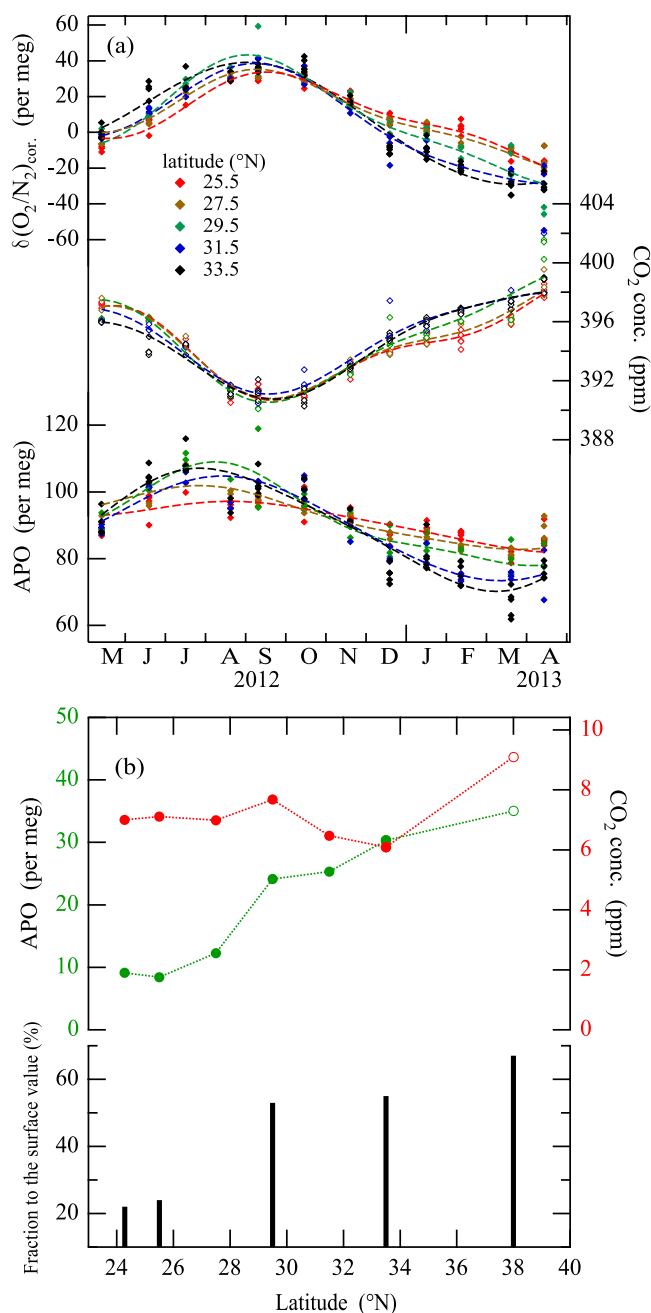


Fig. 6. (a)  $\delta(\text{O}_2/\text{N}_2)_{\text{cor.}}$ ,  $\text{CO}_2$  concentration and APO observed at height interval between 5.1–6.9 km at each latitude over the western North Pacific. Best-fitted curves to the data consist of two-harmonics and the same linear trends as those used in Fig. 5 are also shown (see text). (b) Latitudinal distributions of peak-to-peak amplitude of the seasonal APO and  $\text{CO}_2$  concentration cycles observed in this study (closed circles) and those at 4 km over Sendai, Japan (Ishidoya et al. 2012b) (open circles). Ratios of the seasonal APO amplitude in the middle troposphere to the surface value at respective latitudes are also shown. The surface seasonal APO amplitudes are from the values at 0.0–1.7 km over MNM (this study), at 25, 30 and 35°N over the western Pacific (Fig. 9 in Tohjima et al. 2012) and in the suburbs of Sendai (Ishidoya et al. 2012b).

itudinal decrease in the ratio is not observed in the seasonal  $\text{CO}_2$  concentration amplitude.

This difference in the spatial distribution of  $\text{O}_2$  and  $\text{CO}_2$  is attributable to the combined effect of the differences in the distribution of the surface seasonal  $\text{O}_2$  and  $\text{CO}_2$  fluxes and their atmospheric transport. The strength of the northern and the southern hemispheric seasonal air-sea  $\text{O}_2$  flux that generates the

seasonal APO cycle is similar but out of phase (Garcia and Keeling 2001). Therefore, compared to the surface, the seasonal APO cycle in the middle troposphere at the northern low latitudes is noticeably reduced by a superposition of the anti-phase seasonal APO cycles, since the inter-hemispheric mixing of air through the Intertropical Convergence Zone (ITCZ) is more significant in the upper troposphere than near the surface (Nakazawa et al. 1991; Matsueda et al. 2002). On the other hand, the surface  $\text{CO}_2$  flux in the southern hemisphere is much smaller than that in the northern hemisphere, resulting in a small seasonal  $\text{CO}_2$  concentration cycle in the southern hemisphere; this will not affect the seasonal  $\text{CO}_2$  cycle in the middle troposphere at northern low latitudes significantly due to the inter-hemispheric air mixing. As a consequence, observations of the seasonal APO cycle in the free troposphere over the subtropical region will be a useful constraint in evaluating the atmospheric transport processes related to the inter-hemispheric mixing of air.

## Acknowledgements

We would like to acknowledge many staffs of Japan Ministry of Defence for supporting the C-130H aircraft observation.

## References

- Bender, M., T. Sowers, and L. Labeyrie, 1994: The Dole effect and its variations during the last 130,000 years as measured in the Vostok ice core. *Global Biogeochem. Cycles*, **8**(3), 363–376.
- Bender, M. L., D. T. Ho, M. B. Hendricks, R. Mika, M. O. Battle, P. P. Tans, T. J. Conway, B. Sturtevant, and N. Cassar, 2005: Atmospheric  $\text{O}_2/\text{N}_2$  changes, 1993–2002: Implications for the partitioning of fossil fuel  $\text{CO}_2$  sequestration. *Global Biogeochem. Cycles*, **19**, GB4017, doi:10.1029/2004GB002410.
- Blaine, T. W., R. F. Keeling, and W. J. Paplawsky, 2006: An improved inlet for precisely measuring the atmospheric  $\text{Ar}/\text{N}_2$  ratio. *Atmos. Chem. Phys.*, **6**, 1181–1184.
- Cassar, N., G. A. Mckinley, M. L. Bender, R. Mika, and M. Battle, 2008: An improved comparison of atmospheric  $\text{Ar}/\text{N}_2$  time series and paired ocean-atmosphere model predictions. *J. Geophys. Res.*, **113**, D21122, doi:10.1029/2008JD009817.
- Draxler, R. R., and G. D. Rolph, 2003: HYSPLIT (HYbrid Single-Particle Lagrangian Integrated Trajectory) Model access via NOAA ARL READY Website (<http://www.arl.noaa.gov/HYSPLIT.php>). NOAA Air Resources Laboratory, Silver Spring, MD.
- Garcia, H., and R. Keeling, 2001: On the global oxygen anomaly and air-sea flux. *J. Geophys. Res.*, **106** (C12), 31155–31166.
- Ishidoya, S., and S. Murayama, 2014: Development of high precision continuous measuring system of the atmospheric  $\text{O}_2/\text{N}_2$  and  $\text{Ar}/\text{N}_2$  ratios and its application to the observation in Tsukuba, Japan. *Tellus*, **66B**, 22574, <http://dx.doi.org/10.3402/tellusb.v66.22574>.
- Ishidoya, S., S. Morimoto, S. Aoki, S. Taguchi, D. Goto, S. Murayama, and T. Nakazawa, 2012a: Oceanic and terrestrial biospheric  $\text{CO}_2$  uptake estimated from atmospheric potential oxygen observed at Ny-Alesund, Svalbard, and Syowa, Antarctica. *Tellus*, **64B**, 18924, <http://dx.doi.org/10.3402/tellusb.v64i0.18924>.
- Ishidoya, S., S. Aoki, D. Goto, T. Nakazawa, S. Taguchi, and P. K. Patra, 2012b: Time and space variations of the  $\text{O}_2/\text{N}_2$  ratio in the troposphere over Japan and estimation of global  $\text{CO}_2$  budget. *Tellus*, **64B**, 18964, <http://dx.doi.org/10.3402/tellusb.v64i0.18964>.
- Ishidoya, S., S. Sugawara, S. Morimoto, S. Aoki, T. Nakazawa, H. Honda, and S. Murayama, 2013: Gravitational separation in the stratosphere – a new indicator of atmospheric circulation. *Atmos. Chem. Phys.*, **13**, 8787–8796, 2013, [www.atmoschem-phys.net/13/8787/2013/](http://www.atmoschem-phys.net/13/8787/2013/), doi:10.5194/acp-13-8787-2013.

- Keeling, R. F., and S. R. Shertz, 1992: Seasonal and interannual variations in atmospheric oxygen and implications for the global carbon cycle. *Nature*, **358**, 723–727.
- Keeling, R. F., A. C. Manning, E. M. McEvoy, and S. R. Shertz, 1998: Methods for measuring changes in atmospheric O<sub>2</sub> concentration and their application in southern hemisphere air. *J. Geophys. Res.*, **103**, 3381–3397.
- Keeling, R. F., T. Blaine, B. Paplawsky, L. Katz, C. Atwood, and T. Brockwell, 2004: Measurement of changes in atmospheric Ar/N<sub>2</sub> ratio using a rapid-switching, single-capillary mass spectrometer system. *Tellus*, **56B**, 322–338.
- Langenfelds, R. L., R. Francey, L. P. Steele, R. F. Keeling, M. Bender, M. Battle, and W. F. Budd, 1999: Measurements of O<sub>2</sub>/N<sub>2</sub> ratio from the Cape Grim air archive and three independent flask sampling program. *Baseline atmospheric program (Australia)*, **1996**, 57–70.
- Machta, L., and E. Hughes, 1970: Atmospheric oxygen in 1967 to 1970. *Science*, **168**, 1582–1584.
- Manning, A. C., and R. F. Keeling, 2006: Global oceanic and terrestrial biospheric carbon sinks from the Scripps atmospheric oxygen flask sampling network. *Tellus*, **58B**, 95–116.
- Matsueda, H., H. Y. Inoue, and M. Ishii, 2002: Aircraft observation of carbon dioxide at 8–13 km altitude over the western Pacific from 1993 to 1999. *Tellus*, **54B**, 1–21, doi:10.1034/j.1600-0889.2002.00304.x.
- Nakazawa, T., K. Miyashita, S. Aoki, and M. Tanaka, 1991: Temporal and spatial variations of upper tropospheric and lower stratospheric carbon dioxide. *Tellus*, **43B**, 106–117.
- Niwa, Y., K. Tsuboi, H. Matsueda, Y. Sawa, T. Machida, M. Nakamura, T. Kawasato, K. Saito, S. Takatsuji, K. Tsuji, H. Nishi, K. Dehara, Y. Baba, D. Kuboike, S. Iwatsubo, H. Ohmori, and Y. Hanamiya, 2014: Seasonal Variations of CO<sub>2</sub>, CH<sub>4</sub>, N<sub>2</sub>O and CO in the Mid-troposphere over the Western North Pacific Observed using a C-130H Cargo Aircraft. *J. Meteorol. Soc. Japan*, **92(1)**, doi:10.2151/jmsj.2014-104.
- Rolph, G. D., 2003: Real-time Environmental Applications and Display sYstem (READY) Website (<http://www.arl.noaa.gov/ready.php>), NOAA Air Resources Laboratory, Silver Spring, MD.
- Severinghaus, J., 1995: Studies of the terrestrial O<sub>2</sub> and carbon cycles in sand dune gases and in biosphere 2. *Ph. D. thesis, Columbia University*, New York.
- Stephens, B. B., R. F. Keeling, and W. J. Paplawsky, 2003: Shipboard measurements of atmospheric oxygen using a vacuum-ultraviolet absorption technique. *Tellus*, **55B**, 857–878.
- Stephens, B. B., P. S. Bakwin, P. P. Tans, R. M. TecLaw, and D. Baumann, 2007: Application of a differential fuel-cell analyzer for measuring atmospheric oxygen variations. *Journal of Atmos. and Oceanic Tech.*, **24**, 82–94.
- Stephens, B. B., R. F. Keeling, M. Heimann, K. Six, R. Murnane, and K. Caldeira, 1998: Testing global ocean carbon cycle models using measurements of atmospheric O<sub>2</sub> and CO<sub>2</sub> concentration. *Global Biogeochem. Cycles*, **12(2)**, 213–230.
- Stephens, B. B., S. R. Shertz, A. S. Watt, J. D. Bent, R. F. Keeling, S. C. Wofsy, B. C. Daube, R. Jimenez, E. A. Kort, and S. E. Mikaloff-Fletcher, 2009: Airborne observation of atmospheric O<sub>2</sub> and CO<sub>2</sub> on regional to global scales. *Proceedings (CD) of 8th International Carbon Dioxide Conference*, Jena, Germany, September 13–19, 2009.
- Sturm, P., M. Leuenberger, J. Moncrieff, and M. Ramonet, 2005: Atmospheric O<sub>2</sub>, CO<sub>2</sub> and δ<sup>13</sup>C measurements from aircraft sampling over Griffin Forest, Perthshire, UK. *Rapid Commun. Mass Spectrom.*, **19**, 2399–2406, doi:10.1002/rcm.2071.
- Sturm, P., M. Leuenberger, F. L. Valentino, B. Lehmann, and B. Ihly, 2006: Measurements of CO<sub>2</sub>, its isotopes, O<sub>2</sub>/N<sub>2</sub>, and <sup>222</sup>Rn at Bern, Switzerland. *Atmos. Chem. Phys.*, **6**, 1991–2004.
- Tohjima, Y., H. Mukai, T. Machida, and Y. Nojiri, 2003: Gas-chromatographic measurements of the atmospheric oxygen/nitrogen ratio at Hateruma Island and Cape Ochi-Ishi, Japan. *Geophys. Res. Lett.*, **30**, 1653, doi:10.1029/2003GL01782.
- Tohjima, Y., H. Mukai, T. Machida, Y. Nojiri, and M. Gloor, 2005: First measurements of the latitudinal atmospheric O<sub>2</sub> and CO<sub>2</sub> distributions across the western Pacific. *Geophys. Res. Lett.*, **32**, L17805, doi:10.1029/2005GL023311.
- Tohjima, Y., C. Minejima, H. Mukai, T. Machida, H. Yamagishi, and Y. Nojiri, 2012: Analysis of seasonality and annual mean distribution of the atmospheric potential oxygen (APO) in the Pacific region. *Global Biogeochem. Cycles*, **26**, GB4008, doi:10.1029/2011GB004110.
- Tsuboi, K., H. Matsueda, Y. Sawa, Y. Niwa, M. Nakamura, D. Kuboike, K. Saito, H. Ohmori, S. Iwatsubo, H. Nishi, Y. Hanamiya, K. Tsuji, and Y. Baba, 2013: Evaluation of a new JMA aircraft flask sampling system and laboratory trace gas analysis system. *Atoms. Meas. Tech.*, **6**, 1257–1270, doi:10.5194/amt-6-1257-2013.
- Wada, A., H. Matsueda, Y. Sawa, K. Tsuboi, and S. Okubo, 2011: Seasonal variation of enhancement ratios of trace gases observed over 10 years in the western North Pacific. *Atmospheric Environment*, **45**, 2129–2137, doi:10.1016/j.atmosenv.2011.01.043.
- Wada, A., H. Matsueda, S. Murayama, S. Taguchi, S. Hirao, H. Yamazawa, J. Moriizumi, K. Tsuboi, Y. Niwa, and Y. Sawa, 2013: Quantification of emission estimates of CO<sub>2</sub>, CH<sub>4</sub> and CO for East Asia derived from atmospheric radon-222 measurements over the western North Pacific. *Tellus*, **65B**, 18037, doi:10.3402/tellusb.v65i0.18037.

Manuscript received 19 November 2013, accepted 27 January 2014  
 SOLA: <http://www.jstage.jst.go.jp/browse/sola/>